A review of exfoliated graphite

D. D. L. Chung

Journal of Materials Science
Full Set - Includes `Journal of Materials Science Letters'

ISSN 0022-2461
Volume 51
Number 1

J Mater Sci (2016) 51:554-568
DOI 10.1007/s10853-015-9284-6

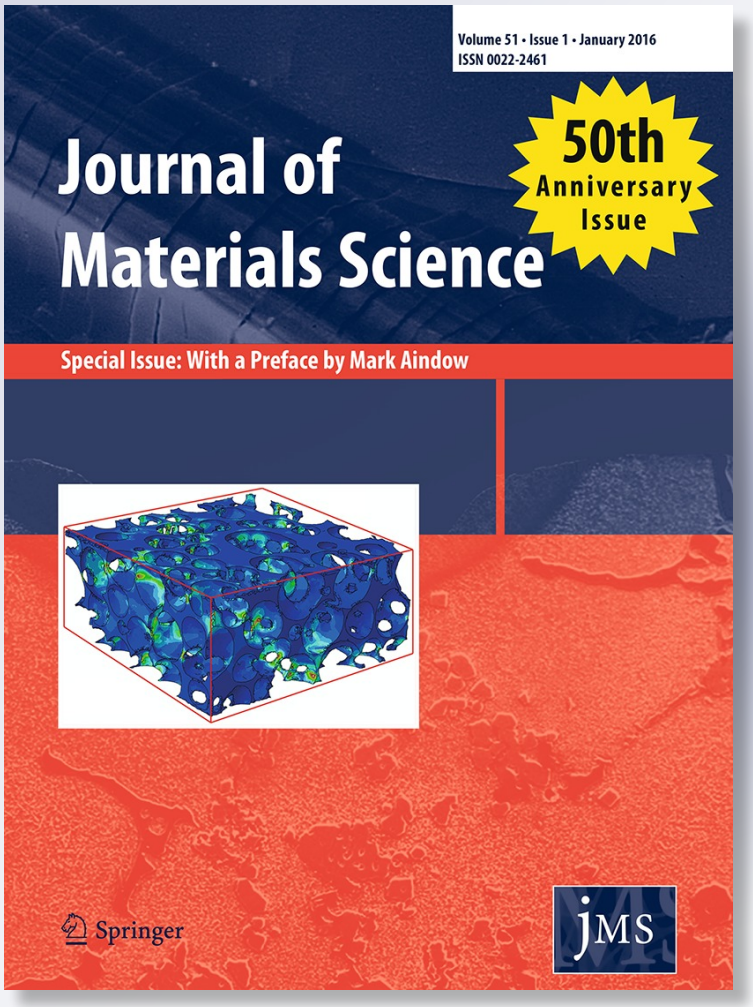

Springer

J Mater Sci (2016) 51:554–568
DOI 10.1007/s10853-015-9284-6

50TH ANNIVERSARY

A review of exfoliated graphite

D. D. L. Chung[1]

Received: 6 June 2015 / Accepted: 20 July 2015 / Published online: 26 July 2015

Abstract Exfoliated graphite (EG) refers to graphite that has a degree of separation of a substantial portion of the carbon layers in the graphite. Graphite nanoplatelet (GNP) is commonly prepared by mechanical agitation of EG. The EG exhibits clinginess, due to its cellular structure, but GNP does not. The clinginess allows the formation of EG compacts and flexible graphite sheet without a binder. The exfoliation typically involves intercalation, followed by heating. Upon heating, the intercalate vaporizes and/or decomposes into smaller molecules, thus causing expansion and cell formation. The sliding of the carbon layers relative to one another enables the cell wall to stretch. The exfoliation process is accompanied by intercalate desorption, so that only a small portion of the intercalate remains after exfoliation. The most widely used intercalate is sulfuric acid. The higher concentration of residue in unwashed EG causes the relative dielectric constant (50 Hz) of the EG to be 360 (higher than 120 for KOH-activated GNP), compared to the value of 38 for the water-washed case. An EG compact is obtained by the compression of EG at a pressure lower than that used for the fabrication of flexible graphite. Compared to flexible graphite, EG compacts are mechanically weak, but they exhibit viscous character, out-of-plane electrical/thermal conductivity and liquid permeability. The viscous character (flexural loss tangent up to 35 for the solid part of the compact) stems from the sliding of the carbon layers relative to one another, with the ease of the sliding enhanced by the exfoliation process.

Introduction

Exfoliated graphite (EG) refers to graphite that has a degree of separation of a substantial portion of the carbon layers in the graphite. The process that results in this separation is known as exfoliation [1], which can involve chemical, mechanical, and thermal methods. The separation occurs between adjacent carbon layers, but typically not all the carbon layers are separated. The separation may or may not occur throughout the entire plane between the adjacent carbon layers.

In case that the separation does not occur throughout the entire plane, the graphite remains intact as a single piece, with local separation of the layers in parts of various planes between carbon layers. The distributed local separation of the layers typically results in a cellular structure, with the wall of each cell typically consisting of multiple carbon layers (e.g., 60 layers, which correspond to a wall thickness of 20 nm). Due to the porosity associated with the local separation, the volume is increased and the density is decreased relative to graphite that has not been exfoliated. If the porosity includes open porosity due to cell bursting, the specific surface area is also increased.

In case that the separation occurs throughout the entire plane, the graphite is separated into multiple pieces, such that each piece has a small number of carbon layers compared to the graphite before the separation. Because of the small number of carbon layers, which are stacked (with or without the AB stacking order that is characteristic of graphite), the thickness is small (e.g., 15 nm) and the dimension in the plane perpendicular to the thickness is

✉ D. D. L. Chung
ddlchung@buffalo.edu;
http://alum.mit.edu/www/ddlchung

[1] Composite Materials Research Laboratory, State University of New York, University at Buffalo, Buffalo, NY 14260-4400, USA

also small (e.g., 25 μm). If the number of carbon layers is less than 10, the piece is known as graphene. According to the original definition due to Boehm [2], graphene is a material with a single carbon layer. However, the definition has been broadened in recent years and the term "few-layer graphene" is often used. If the number of carbon layers is 10 or more, the piece is known as a graphite nanoplatelet (GNP), also known as an exfoliated graphite nanoplatelet (xGnP) [3], and also known as a graphite nanosheet (GNS). Depending on its thickness, a GNP differs in structure. A GNP of a relatively small size (less than about 50 nm thick) does not exhibit a cellular structure, whereas a GNP of a relatively large size (more than about 50 nm thick) may or may not exhibit a cellular structure.

This review does not address graphene, but focuses on EG that exhibits a cellular structure and on GNP. The former includes EG compacts, which is obtained by the compaction of multiple pieces of EG in the absence of a binder. Due to the cellular structure and the consequent mechanical interlocking among the pieces of EG, the compact is a monolith in the absence of a binder and can be considered a type of carbon foam [4]. In case that the compaction pressure is high, the mechanical locking is strong and a reasonably strong sheet results. This sheet is known as flexible graphite, which is commercially available, being mostly used as a gasket material for the sealing of fluids. In this review, the preparation, structure, properties, and applications are addressed for these materials.

Exfoliated graphite exhibiting a cellular structure

The exfoliation process that gives EG exhibiting a cellular structure is associated with a large expansion (typically exceeding 100 times) along the *c*-axis of the graphite [5–8]. The expansion results in a fluffy morphology.

Most commonly, the graphite prior to exfoliation is in the form of flakes, which have the graphite *c*-axis perpendicular to the plane of the flake. Because of the large expansion along the *c*-axis, the exfoliated flake becomes long in the direction that corresponds to the *c*-axis of the flake prior to exfoliation. As a consequence, the EG made from a graphite flake looks like a worm (Fig. 1) and is known as a worm.

Because of its unusual structure (Fig. 1b), EG exhibits properties (mechanical, thermal, electrical, dielectric, and other properties) that differ from those of conventional graphite and has numerous applications that are beyond those for conventional graphite. These applications include gasketing, electromagnetic interference (EMI) shielding, electrochemical electrodes, vibration damping, adsorption, thermal interfacing, etc.

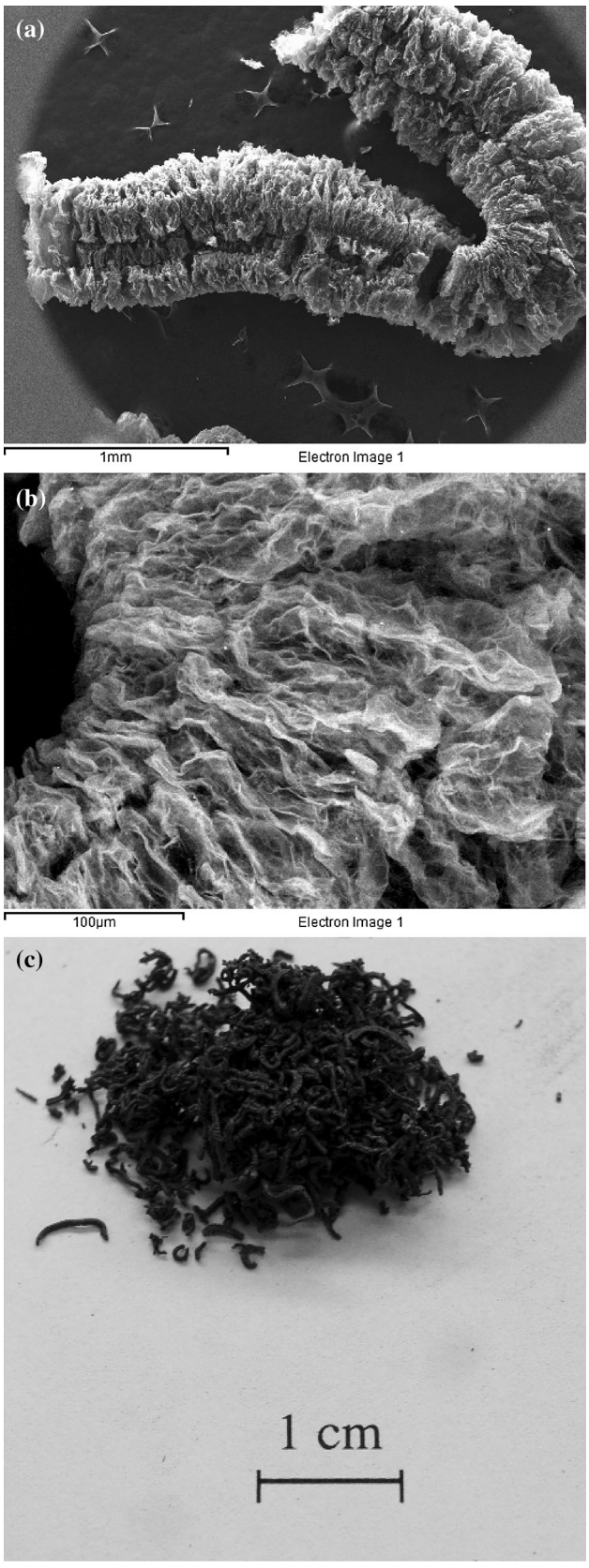

◀**Fig. 1** Exfoliated graphite (made by heating sulfuric-acid-intercalated graphite flake) that has been washed after exfoliation. **a** SEM photograph of exfoliated graphite (essentially an entire worm) at a low magnification [39]. **b** SEM photograph of exfoliated graphite (a part of a worm) at a high magnification [39]. **c** Optical photograph of a collection of worms [32]

Exfoliation of intercalated graphite

The exfoliation of graphite typically involves the intercalation of graphite to form a graphite intercalation compound (GIC, also known as intercalated graphite) [9, 10], followed by heating of the GIC [5, 11]. The intercalation compound is also known as expandable graphite, since it can be exfoliated upon heating.

A GIC is a layered compound with the foreign species (known as the intercalate) between at least some of the carbon layers. The number of carbon layers between adjacent intercalate layers is known as the stage of the intercalation compound. The intercalation process is enabled by the fact that graphite has a layered structure (Fig. 2) and is highly anisotropic, with strong bonding (covalent and metallic bonding) in the plane of the layers and weak bonding (van der Waals' forces) in the direction perpendicular to the layers. The carbon in graphite is sp^2 hybridized. This hybridization is responsible for the trigonal coordination and the consequent planar structure of the layers.

Graphite intercalation compounds are classified into two types, namely the ionic compounds and the covalent compounds. The ionic compounds (e.g., graphite intercalated with sulfuric acid, which is also known as graphite bisulfate) are characterized by charge transfer between the intercalate and the graphite [12], so that a low degree of ionic bonding occurs. It should, however, be emphasized that the degree of ionicity in compounds of this group may be very low. Moreover, many of the intercalates of this group retain their molecular identity in the graphite lattice, so that the nature of the ionic bonding is more complicated than that in many of the totally ionic solids, where simple ions are involved. Although many of the compounds of this group involve such a small degree of ionization that they should not really be called "ionic," they are referred to as ionic intercalation compounds for convenience in classification.

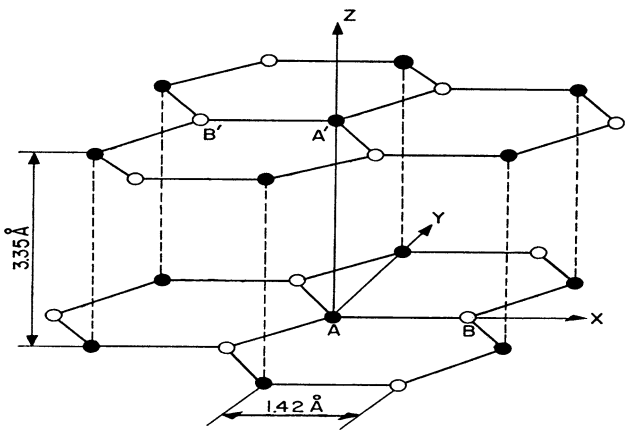

Fig. 2 The crystal structure of graphite [9]

The covalent compounds (e.g., graphite oxide, which is also known as graphite acid) are characterized by covalent bonding between the intercalate and the graphite. In case of graphite oxide (GO, which can be prepared from graphite by chemical, electrochemical, or electrostatic methods [13–15]), the covalent bonding involves the change of the hybridization of some of the carbon from sp^2 to sp^3 and the bonding of the oxygen atoms to the sp^3-hybridized carbon atoms. As a consequence of the sp^3 hybridization and the associated tetrahedral coordination, the carbon layers in GO are not planar and the interplanar spacing is relatively large. As a consequence, the carbon layers in GO can be separated more easily than those in intercalated graphite of the ionic type [16]. Because single layers can be obtained, this route is commonly used to prepare graphene. In contrast, for the intercalated graphite of the ionic type, it is relatively difficult to obtain single layers, partly due to the AB stacking order. The GO may be reduced chemically to remove the oxygen, thereby forming graphite or graphene [17]. However, the reduction process tends to give rise to defects in the carbon layers [18].

A high degree of crystallinity is required for the formation of a GIC of the ionic type. Therefore, natural graphite flakes are most commonly used for preparing EG from these compounds. The exfoliation of carbon fibers is much more difficult, due to the relatively low degree of crystallinity of carbon fibers [7, 19]. The degree of crystallinity of carbon fibers is low compared to that of natural graphite flakes, even for the most graphitic types of carbon fiber.

The structure of a GIC of the ionic type (according to Daumas and Herold [20]) is illustrated in Fig. 3. This model applies to stages greater than 1 and has been confirmed by electron microscopy [21, 22]. Instead of an intercalate layer extending from one end of a graphite crystal to the other, multiple intercalate islands exist, as enabled by the local bending of the carbon layers. Upon heating, the intercalate either vaporizes (due to the relatively low boiling point of the intercalate) [8] or decomposes into smaller molecules [23], thus causing each island to expand like a balloon [6]. Due to the role of the intercalate islands in the process of exfoliation, the degree of exfoliation tends to decrease with decreasing graphite particle size [24].

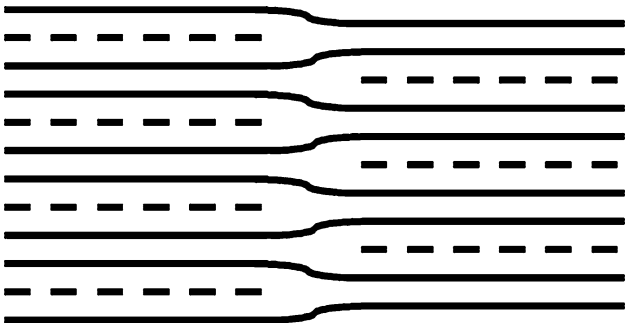

Fig. 3 The structure of a graphite intercalation compound according to Daumas and Herold [20]. The *solid lines* indicate the carbon layers. The *dashed lines* indicate the intercalate layers. The carbon layers are bent at certain locations, thus resulting in intercalate islands between the bend locations. The intercalation compound illustrated here has stage = 2, but the concept applies to any stage [61]

The force required for the sliding of the carbon layers relative to one another is provided by the vaporization or decomposition of the intercalate upon heating. In order to increase this force, so that the degree of expansion is relatively high, the heating rate should be high. The rapid heating can be conducted using furnace heating [24], microwave heating [24–26], or combustion [27].

In order to produce EG that remains exfoliated at room temperature, the exfoliation process needs to be substantially irreversible upon cooling. The irreversibility is enabled by the breaking of a substantial portion of the balloon walls during exfoliation [6]. This breaking requires a sufficiently large increase in volume upon conversion of the intercalate to either its vapor or smaller molecules. Typically, the decomposition of the intercalate into smaller molecules gives rise to a greater volume increase than the mere vaporization of the intercalate. The amount of gas evolved during exfoliation depends on the intercalate species. The exfoliation of graphite intercalated with nitric acid or sulfuric acid tends to be substantially irreversible, whereas the exfoliation of graphite intercalated with bromine tends to be essentially reversible [6]. However, bromine is attractive for the relatively low temperature (500 °C) for its thermal exfoliation [28]. Nitric acid, sulfuric acid, and bromine are all acceptor intercalates, i.e., they accept electrons from the graphite. Since graphite is a semi-metal, this doping causes the graphite to be oxidized, so that the resulting intercalation compound is a hole conductor, i.e., a p-type conductor.

In contrast to the abovementioned oxidative intercalation, non-oxidative intercalation of graphite by Brønsted acids (e.g., phosphoric, sulfuric, dichloroacetic, and alkylsulfonic acids) has recently be reported [29]. The intercalation results in stage-1 GIC along with pristine graphite. Immersion of the GIC in dimethylformamide causes disintegration of the GIC and gives a graphene suspension.

Structure of exfoliated graphite

The expansion associated with exfoliation is enabled by the shear of the carbon layers. The sliding of the carbon layers relative to one another enables the balloon wall to stretch as the island expands to form a balloon. Thus, a cellular structure results [30], with each cell corresponding to a balloon and the cell wall corresponding to the balloon wall [31], as illustrated in Fig. 4. In case of the intercalate being sulfuric acid, the cell wall typically consists of about 60 carbon layers, so that the cell wall thickness is about 20 nm [31].

For a large amount of expansion during exfoliation, a relatively large size of the intercalate islands is preferred. A relatively large island size can be obtained by using a relatively low intercalate activity (such as a relatively low intercalate vapor pressure) during intercalation [6].

The abovementioned breaking of the balloon walls during exfoliation is advantageous for increasing the specific surface area. A high surface area is valuable for applications related to adsorption, electrochemical electrodes, and EMI shielding. Adsorption is relevant to oil removal and phase change material incorporation. Electrochemical applications relate to supercapacitors, batteries, and gas sensors. A high surface area is desirable for shielding, due to the skin effect (the phenomenon in which high-frequency electromagnetic radiation penetrates only the near surface region of an electrical conductor). However, even for the irreversibly exfoliated sulfuric-acid-intercalated graphite, the specific surface area is only about 45 m^2/g [32], which is very low compared to that of activated carbons, for which the specific surface area typically exceeds 1000 m^2/g.

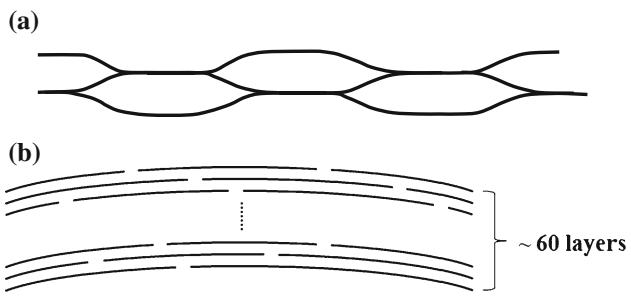

Fig. 4 **a** The cellular structure of exfoliated graphite, with each line representing a cell wall and each cell resulting from an intercalate island. **b** The structure of a cell wall, with each line representing a carbon layer (rather than a cell wall). In the case of exfoliated graphite made from sulfuric-acid-intercalated graphite flakes, the cell wall typically consists of about 60 carbon layers. The substantial sliding between adjacent carbon layers necessitates that each carbon layer in the wall of a given cell wall does not extend from one end of the cell wall to the other; as illustrated, the carbon layers in a cell wall are not continuous [61]

Chemical composition of exfoliated graphite

An intercalation compound tends to desorb a part of its intercalate once it is removed from the reaction vessel in which intercalation is conducted [33]. The higher is the temperature, the faster is the intercalate desorption. Due to the fact that exfoliation is achieved upon heating a GIC, the process of exfoliation is accompanied by extensive desorption of the intercalate, so that only a very small portion of the intercalate in the GIC prior to exfoliation remains after exfoliation. The residual intercalate is strongly held in the EG. The most widely used intercalate species for preparing exfoliated is sulfuric acid. The resulting intercalation compound, known as graphite bisulfate, consists of carbon layers with HSO_4^- radical ions and H_2SO_4 molecules between the layers. This compound is commonly prepared by direct chemical interaction of graphite with a mixture of concentrated sulfuric acid [34] and an oxidizing agent (e.g., nitric acid [34], potassium permanganate, hydrogen peroxide [34], ozone [35], etc.). Similarly, nitric acid can be intercalated [36], with potassium permanganate as an oxidizing agent [37, 38]. However, unlike sulfuric acid, nitric acid can be intercalated without the presence of an oxidizing agent if the concentration of the nitric acid is very high, as in the case of fuming nitric acid. Another method that is effective for the intercalation of sulfuric acid involves electrolysis [34], which is advantageous in that it requires sulfuric acid that is dilute [34]. The residual acidity present in the EG is not desirable for structural applications such as those typically associated with flexible graphite. In order to decrease the residual acidity in the expandable graphite, rinsing with water followed by partial neutralization (i.e., deacidification using an alkaline substance) is commonly conducted. In case of sulfuric acid being the intercalate, the residual sulfur content after the partial neutralization process is typically in the range from 6 to 12 % and surface residues in the form of sulfur compounds and other species due to the intercalation catalyst may exist. On the other hand, the residual intercalate affects the chemistry of the volume (interior) as well as that of the surface of the EG, and such effects may be attractive for electrochemical applications [39, 40].

Although the expandable graphite (sulfuric-acid-intercalated graphite flake) prior to exfoliation has been subjected to rinsing and partial neutralization to remove the residual acidity, the amount of surface residue on the EG is lower if the EG has been subjected to washing by water. Figure 1 shows SEM photographs of washed EG, whereas Fig. 5 shows corresponding photographs of the unwashed material [39]. The surface morphology of the unwashed material is blocky, with the cellular structure not very clear when viewed from the surface (Fig. 5). In contrast, the cellular structure is very clear for the washed material

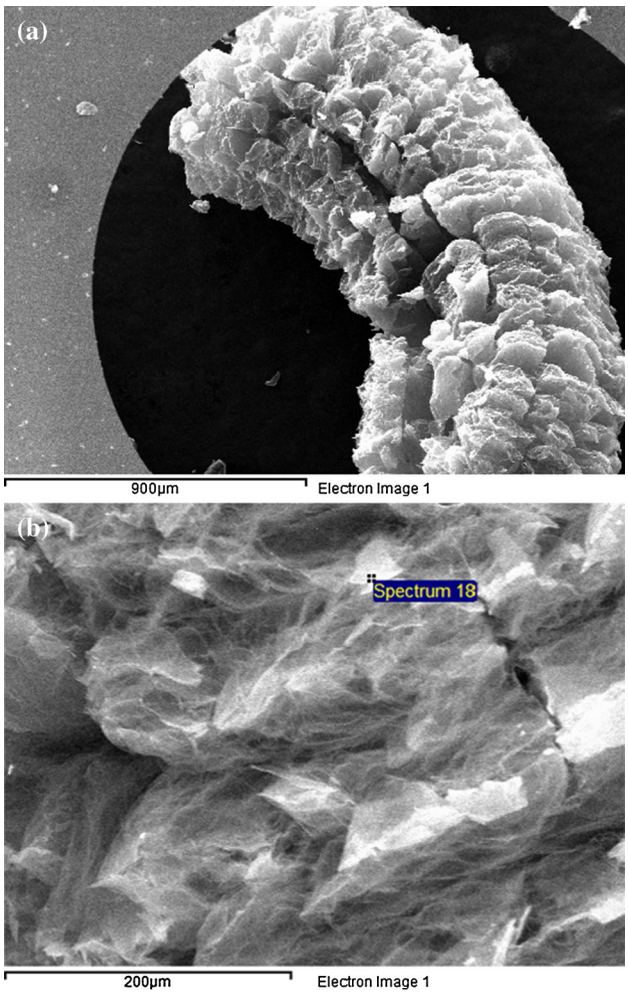

Fig. 5 SEM photographs of exfoliated graphite (made by heating sulfuric-acid-intercalated graphite flake) that has not been washed after exfoliation. **a** Low-magnification view. **b** High-magnification view [39]

when viewed from the surface (Fig. 1). The higher concentration of surface residue in the unwashed case causes the relative dielectric constant (50 Hz) of the EG to be 360, compared to the value of 38 for the washed case [32]. However, the electrical conductivity (50 Hz) is similar at 50 S/m for both washed and unwashed cases [39]. Furthermore, the unwashed material provides a better interface between the EG and an electrical contact (copper), as shown by much lower interfacial resistivity and much higher interfacial capacitance. It should be noted that an interface with the electrical contact is in series with the volume of the EG material, and as a result, the capacitance of this interface is less influential if it is high. That the unwashed material gives a better interface with the electrical contact is attributed to the mechanical fragility of the worms and the possible decrease of the degree of fluffiness of the worms after the washing. The high dielectric constant and the high specific interface capacitance make the

unwashed form potentially attractive for use in supercapacitor electrodes. The relative dielectric constant of 360 for the unwashed EG is even higher than the corresponding value of 120 for potassium-hydroxide-activated GNP [32].

Due to the residual impurity associated with sulfuric acid intercalation, which requires an oxidizing agent such as potassium permanganate, it is attractive to use perchloric acid ($HClO_4$) as the intercalate. Perchloric acid does not require an oxidizing agent for the intercalation process and the exfoliation can be carried out at a relatively low temperature (200 °C) [41].

The EG obtained by the exfoliation of graphite intercalated with nickel chloride ($NiCl_2$) exhibits high hydrogen sorption/desorption capacity. This is partly due to the porous structure and partly due to the dispersed nickel oxide [42].

Chemical functionalization can be conducted to modify the surface chemistry of EG. For example, the functionalization can be used to provide oxygen-containing functional groups on the surface [43]. Functional groups are important for the use of EG for adsorption [25]. Adsorption of oil [26], rhodamine B [25], and 4-chlorophenol [25] has been reported. Functionalization of the edge of the carbon layers with the carboxyl group enhances the formation of self-assembled EG structures in a polymer–matrix composite [44]. The doping of EG with nitrogen and sulfur (by the pyrolysis of a mixture of EG and an ionic liquid) provides a metal-free catalyst for the oxygen reduction reaction, which is relevant to fuel cells [45]. The volume of the EG (not just the surface) can be modified by fluorination [46].

The impregnation of EG with cobalt ferrite increases the proportion of large pores exceeding 1000 nm in size, thereby enhancing the sorption capacity of engine oil [47]. Due to the magnetic character rendered by the cobalt ferrite, the EG that has absorbed the oil can be removed by using a magnet.

Flexible graphite

Flexible graphite [48–55] refers to a graphite sheet that is obtained by the compaction of a collection of worms. The compaction can be performed by rolling [56] or unidirectional compression. The rolling method is suitable for large-scale manufacturing of sheets in roll form. In contrast, compression gives sheets of limited size.

Due to the cellular structure of each worm, the compaction results in mechanical interlocking of the adjacent worms, thereby resulting in a sheet in the absence of a binder. Mechanical deformation of flexible graphite seems to involve units that appear as worms [57]. Because of the sheet is flexible (though not crimpable), it is known as flexible graphite. The greater is the degree of exfoliation of the worms, the higher is the tensile strength of the flexible graphite in the plane of the sheet [49] and the greater is the ability to attenuate electromagnetic radiation in the radio wave regime [37]. In order for the mechanical interlocking between the worms to be strong, the pressure used in the compaction needs to be sufficiently high (e.g., 20–200 MPa [49]). The lower is the pressure, the lower are the density, the tensile strength (in the plane of the sheet), and the degree of preferred orientation of the carbon layers in the sheet.

The thickness of commercially available flexible graphite sheets typically ranges from 0.1 to 2 mm. Thicker sheets tend to break apart in the plane of the sheet after fabrication by compaction of the worms.

Due to the fluffiness of the worms and the consequent huge reduction in volume during the compaction, the carbon layers of the worms in the compact exhibit preferred orientation in the plane of the sheet. Because of this preferred orientation, the electrical/thermal conductivity is higher in the plane of the sheet than in the direction perpendicular to the sheet. Because of this preferred orientation and the cellular structure of the worms, the sheet is resilient in the direction perpendicular to the sheet. This resiliency is valuable for flexible graphite to function as (i) a gasket material for fluids (including fluids in harsh chemical or thermal environments, as relevant to asbestos replacement) [27], (ii) an EMI gasket material (the EMI shielding effectiveness as high as 130 dB at 1 GHz [52–55]), (iii) a thermal interface material (abbreviated TIM, due to the enhanced conformability provided by the resiliency and the need for the TIM to conform to the surface topography of the sandwiching surfaces) [58], and (iv) a vibration damping material (due to the viscous behavior of the sheet, as discussed in "Viscous and elastomeric behavior" section) [52].

The density of ideal graphite is 2.26 g/cm^3; that of commercial flexible graphite is typically around 1.1 g/cm^3 [53]. For commercial flexible graphite, the tensile strength in the plane of the sheet is typically 5.2 MPa, the out-of-plane compressive stress for 10 % reduction in thickness is typically 3.9 MPa, and the coefficient of thermal expansion (CTE) is typically around -0.4×10^{-6}/°C [53].

A lower degree of preferred orientation results in a lower degree of anisotropy, i.e., a lower value of the ratio of the electrical/thermal conductivity in the plane of the sheet to that in the direction perpendicular to the plane [49]. Thus, the in-plane thermal conductivity increases with increasing degree of preferred orientation. A typical value of the in-plane thermal conductivity of commercial flexible graphite is 43 W/(m K) and this corresponds to an out-of-plane thermal conductivity of 3 W/(m K) [53]. However, in-plane thermal conductivity as high as

1500 W/(m K) has been reached [59], though this high in-plane thermal conductivity corresponds to low out-of-plane thermal conductivity. The high in-plane thermal conductivity is attractive for the use of the flexible graphite as a heat spreader [59], which is needed for the cooling of microelectronics. However, high out-of-plane thermal conductivity is needed for heat removal in the out-of-plane direction.

Due to its moderate in-plane electrical conductivity (at a level that is suitable for resistance or Joule heating), high-temperature resistance (900 °C in air), and flexibility, flexible graphite is used as a heating element [51]. The flexibility facilitates its implementation. In contrast, conventional graphite is not flexible, though it is commonly used as a heating element in high-temperature furnaces.

The surface modification of flexible graphite by using superheated steam increases the in-plane thermal diffusivity [56]. In addition, the treatment of flexible graphite with fluorine enhances the gas permeability in relation of hydrogen, carbon dioxide, nitrogen, and oxygen [60].

Exfoliated graphite compacts

An EG compact refers to a compact obtained by the compression of worms such that the pressure is considerably lower than that typically used for the fabrication of flexible graphite ("Flexible graphite" section). For example, the pressure used for making EG compacts ranges from 0.71 to 11.7 MPa, thus resulting in density ranging from 0.047 to 0.67 g/cm^3, and solid content ranging from 2.1 to 30 vol% [61]. Due to the low degree of compaction compared to flexible graphite, EG compacts are mechanically weak compared to flexible graphite. However, they exhibit viscous character, out-of-plane electrical/thermal conductivity, and liquid permeability that are much greater than those of flexible graphite. This section addresses the mechanical, thermal, electrical, adsorption, and filtration behavior of these compacts.

Viscous and elastomeric behavior

The force during exfoliation irreversibly loosens the bond between the carbon layers, so that the ease of sliding between the layers is irreversibly increased. As a consequence of the enhanced ease of sliding and the large area of the interface between the carbon layers in a cell wall (Fig. 4), EG exhibits strong viscous behavior under dynamic strain [31, 62] and elastomeric behavior under static strain [63]. The viscous behavior and elastomeric behavior are valuable for vibration damping and vibration isolation, respectively. The sliding enables the stretching of the cell wall, which occurs during mechanical deformation, as illustrated in Fig. 6. This interface-derived viscous mechanism is in contrast to the well-known bulk viscous deformation mechanism that rubber exhibits. Even though the amplitude of the sliding may be small under dynamic loading, the sliding is easy and the back-and-forth sliding during vibration provides a significant degree of viscous behavior. It is akin to the wall of a balloon stretching and recoiling at a small deformation amplitude during repeated variation in the gas pressure in the balloon. Thus, the cell wall of EG provides balloon-like interface-derived viscous behavior. The degree of viscous character is described by the loss tangent (i.e., tan δ, where δ is the phase lag between the stress wave and the strain wave during dynamic loading), which is equal to the ratio of the loss modulus to the storage modulus. The viscous behavior of the cell wall is associated with loss tangent as high as 35 under dynamic flexure and as high as 25 under dynamic compression of the EG compact [31]. Both values of 35 and 25 are unprecedentedly high values among solid materials. The values decrease with increasing degree of compaction of the EG (i.e., with increasing solid content in the compact) (Fig. 7), due to the associated decreasing ease of sliding between the layers as the compact becomes more tightly packed. This means that an adequate degree of looseness of the binding between the layers is required for the viscous behavior to be substantial. In contrast to EG, the loss tangent is only 0.7 for rubber under dynamic flexure [64]. The reversibility of the elastomeric deformation of the cell wall is believed to stem from the pinning of the cell wall at its extremities (Fig. 4). The pinning is akin to the intermolecular crosslinking that enables the reversible elastomeric character of rubber.

Due to the strong viscous character of the cell wall, the incorporation of EG in a stiff material such as cement provides constrained-layer damping in the microscale,

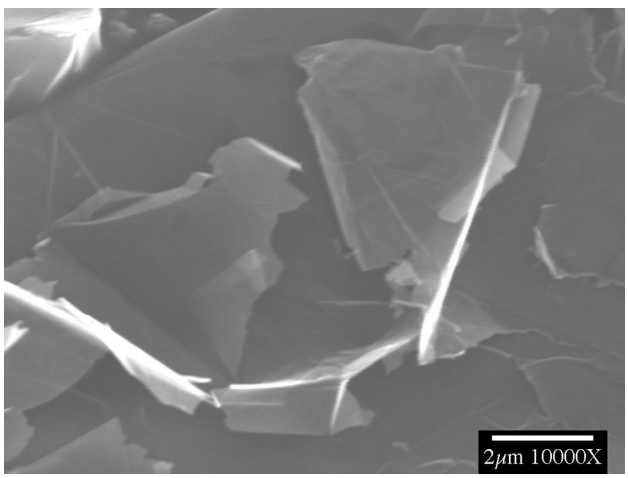

Fig. 6 SEM photograph of graphite nanoplatelet [70]

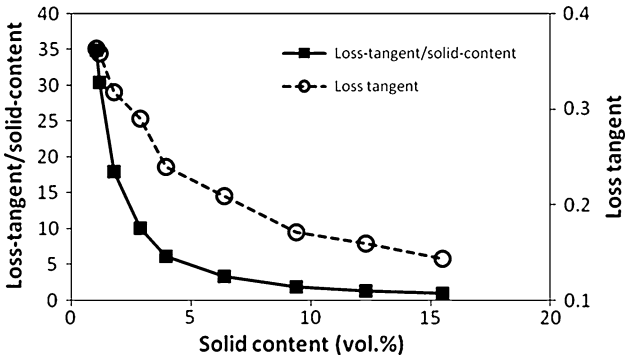

Fig. 7 Dynamic flexural properties of exfoliated graphite compacts at various solid contents (solid volume fractions), with the static strain at 2 %. The loss tangent divided by the solid content relates to the degree of viscous character of the cell wall; its highest value of 35 occurs at the lowest solid content of 1 vol % [31]

provided that the sandwiching of the EG by the stiff matrix material of the composite is tight enough [65, 66]. These cement–matrix composites are covered in "Exfoliated graphite composites" section.

Electrical and thermal conduction behavior

Increase of the compaction pressure enhances the in-plane electrical/thermal conductivity at the expense of the out-of-plane electrical/thermal conductivity. The highest out-of-plane thermal and electrical conductivities reported for the graphite part of the EG compact (with the air contribution excluded by calculation) are 550 W/(m K) and 230 kS/m, respectively [61]. These values indicate that graphite *a*-axis conduction (rather than *c*-axis conduction) contributes primarily to the out-of-plane conduction in an EG compact. The out-of-plane thermal and electrical conductivities correlate linearly, in accordance with the Wiedemann–Franz Law, because both thermal conduction and electrical conduction are governed by the degree of preferred orientation [61]. The compaction-related variation in the solid-part conductivities is large [21–550 W/(m K) and 10–230 kS/m, respectively], due to the preferred orientation variation [61]. The out-of-plane Lorentz number (7.3×10^{-6} W Ω/K^2) is similar to the in-plane value, being independent of the preferred orientation [35]. At 2–7 vol% solid in the EG compact, out-of-plane thermal conductivity and electrical conductivity of 7 W/(m K) and 3 kS/m, respectively, are obtained for the overall compact [61]. These values are toward the targets for fuel cell bipolar plates. The higher is the packing density of the EG compact, the greater is the degree of anisotropy in the thermal conductivity between the in-plane and out-of-plane directions of the compact, as shown for the case of the intercalate being nitric acid [67].

Adsorption and filtration behavior

An EG compact with a low density of 0.025 g/cm^3 is effective to function as a filter for the treatment of oilfield-produced water, while providing adequate strength [68]. The higher is the density, the greater is the strength, but the lower is the permeability. The density of 0.025 g/cm^3 corresponds to a compromise between these two opposing properties.

An EG compact modified with a poly(propylene imine) dendrimer by electrodeposition provides an electrochemical sensor for lead in water [69]. An unmodified EG compact under an applied potential provides the removal of lead ions from water [69].

Graphite nanoplatelet

Adequate mechanical agitation of EG (e.g., by sonication) can disintegrate the worms, thereby resulting in a form of nanographite known as GNP (Fig. 6) [70]. As shown in Fig. 6, there is no cellular structure. GNP is not graphene, because the number of carbon layers in a platelet can be quite large (much greater than 10). It is particulate, but it is not fluffy.

The worms can cling to one another in the absence of a binder (Fig. 1c). This clinginess is attractive for applications (such as electrochemical electrodes) for which a binder is detrimental to the functional performance. In contrast, GNP does not exhibit this clinginess. Nevertheless, a mixture of GNP and worms is clingy, due to the worms. In other words, the worms serve as a carrier for the GNP [32].

GNP paper prepared by vacuum filtration exhibits in-plane thermal conductivity 180 W/(m K) and out-of-plane thermal conductivity 1.3 W/(m K) [71]. The in-plane thermal conductivity is much lower than that of flexible graphite (as high as 1500 W/(m K) [59]).

Most research on GNP pertains to composite materials. The GNP composites are addressed in "Graphite nanoplatelet composites" section.

Composites

This section addresses EG composites, flexible graphite composites, and GNP composites. The composites include polymer–matrix, carbon–matrix, cement–matrix, and metal–matrix composites. In addition, they include liquid-based dispersions of the graphite and graphite coated with other materials.

Exfoliated graphite composites

The EG can be used as a filler in composites. The primary applications relate to electrical and thermal conduction, which benefit from the connectivity provided by the EG microstructure.

The addition of EG to polypropylene gives a polymer–matrix composite with increased values of the flexural modulus and storage modulus, while the impact strength is essentially unaffected [72]. Due to the electrical and thermal conductivity of EG, the incorporation of EG in phenolic gives a polymer–matrix composite that is attractive for use as the bipolar plate of a polymer electrolyte membrane fuel cell [73]. The incorporation of EG in a polymer is also attractive for increasing the EMI shielding effectiveness [74, 75]. However, the shielding effectiveness is considerably lower than that of flexible graphite [52–55].

EG surrounded by a polystyrene superhydrophobic membrane (which is like a teabag) has been reported to be effective for the adsorption of oil [76]. The main application relates to oil spill cleanup.

The addition of EG to an elastomer in the form of poly(dimethylsiloxane), which is electrically insulating, increases the electrical conductivity to values up to 0.4 S/cm, thereby providing a compliant electrode material [77]. The incorporation of EG in a polyimide film is associated with a percolation threshold of 3.1 vol% [78]. The addition of a polyaniline fibers to the surface of EG prior to incorporation in poly(vinylidene fluoride) gives a polymer–matrix composite with relative dielectric constant 17 and dielectric loss 0.06 at 1 kHz [79]. The low loss is attributed to the non-conductive fibers causing the EG units not to touch one another in the composite.

Manganese dioxide (MnO_2) is a common active electrochemical electrode material. The EG combined with MnO_2 to form a nanostructure has been reported to be effective as an electrode material for supercapacitors [80, 81]. The addition of EG to MnO_2 increases the energy density relative to the case without EG [80].

EG incorporated in a carbon–matrix composite gives a graphite foam [82]. This is achieved by adding expandable graphite to pitch, which is subsequently carbonized while exfoliation occurs. In another process, the carbonization of an organic foam containing EG gives a carbon foam, which is suitable for hosting phase change materials [83]. An EG compact subjected to chemical vapor infiltration (CVI) of a carbon precursor, followed by carbonization of the precursor, gives a carbon–matrix composite [84].

The incorporation of EG in a cement–matrix composite provides strong ability for vibration damping [65, 66]. In order for the cell wall of EG to be sufficiently tightly sandwiched by the cement matrix, as needed for constrained-layer damping, the fabrication of the cement-based material requires compaction prior to curing. A process involves dry compaction of a mixture of cement particles and EG prior to exposure to water for curing the cement [65]. Simple addition of the EG to a cement mix does not provide the necessary squeezing, thus resulting in loose sandwiching of the EG by the cement matrix after curing and the near absence of constrained-layer damping [66]. Furthermore, without the squeezing, the EG units (worms) in the cement remain macroscopic and highly porous, making them ineffective for enhancing the strength. In contrast, with the squeezing, the EG is effective for enhancing the strength. Thus, the method of incorporating EG in cement is critical. In practice, the squeezing may be achieved by using roller compaction.

Even with the tight incorporation of EG in a cement–matrix composite, the elastic modulus (relative to that of cement without graphite) is decreased by the incorporation. This issue can be circumvented by the combined use of EG and silica fume, which is an admixture that decreases the pore size and contributes to the damping due to its nanoparticulate nature [85–87].

Glassy carbon is a common electrochemical electrode material used in electrochemical characterization. The coating of a glassy carbon electrode with EG (applied as a suspension, followed by solvent evaporation) provides an electrochemical sensor for tartrazine [88]. Furthermore, EG is effective as a support for Si-based Li-ion battery anodes [89]. In addition, EG [90, 91] is effective as a catalyst support.

Flexible graphite composites

Due to its monolithic form, flexible graphite is not used as a filler in composites. However, due to its porosity, flexible graphite can be impregnated, thus forming composite materials with flexible graphite as the backbone.

Flexible graphite impregnated with a carbon precursor (polymeric), which is subsequently carbonized, gives a composite with tensile strength higher than that of the unmodified flexible graphite sheet [92]. Flexible graphite impregnated (penetrated) with a carbon black organic-based paste gives a superior TIM [93], because of the high conformability of the carbon black paste and the importance of conformability to the TIM performance. Flexible graphite impregnated with the carbon black paste gives superior TIM performance than flexible graphite coated with the paste [94]. Flexible graphite without the paste is inferior in TIM performance to that with the paste, whether the paste penetrates or coats the flexible graphite [93, 94].

Graphite nanoplatelet composites

The GNP is an attractive distributed filler in composites with various matrices, due to the small size of each GNP unit. However, the discontinuity among GNP units limits the ability to form a network, which is valuable for electrical, electrochemical, and thermal conduction applications. The combination of GNP and CNT gives a hybrid supercapacitor electrode material that is superior to that provided by GNP alone, due to the improved network formation. The specific capacitance is 266 F/g for the former and 185 F/g for the latter [95].

The incorporation of GNP in a polymer (nylon 6, i.e., PA6) fiber gives a composite fiber. The GNP incorporation enhances the tensile modulus, such that acid treatment of the GNP improves the bond between GNP and the nylon matrix [96]. The incorporation of GNP in polyamide (PA12) shows that GNP alters the glass transition temperature and crystallization characteristics of PA12 [97]. On the other hand, the addition of GNP to polypropylene decreases the impact strength [98]. The incorporation of GNP in polycarbonate is associated with a percolation threshold of 4.0 vol% [99]; at 5 vol% GNP (above the threshold), the electrical resistivity remains high at 4.0×10^7 Ω cm and the thermal conductivity remains low at 0.37 W/(m K) [99]. The incorporation of GNP in a polymer hydrogel is potentially attractive for improving the ability of the hydrogel to respond to stimuli [100].

The addition of GNP to epoxy gives a polymer–matrix composite with increased values of the electric permittivity, flexural modulus, and storage modulus [101]. The incorporation of GNP in epoxy gives a polymer–matrix composite exhibiting EMI shielding effectiveness 62 dB at 18 GHz [102]. The combined incorporation of GNP and CNT in polypropylene gives a polymer–matrix composite exhibiting EMI shielding effectiveness 36.5 dB at 1.25 GHz [103]. These values are low compared to the value of 87 dB at 1 GHz for a polymer–matrix composite containing nickel-coated carbon nanofiber [104].

The addition of GNP to polystyrene increases the relative dielectric constant from 2.83 to 36.4 at 1 kHz, due to the creation of a large number of microscale capacitors [105], thus causing the capacitors to be high in dielectric loss. However, the conductivity is increased from 3.8×10^{-10} to 1.5×10^{-7} S/m [105]. The addition of GNP to epoxy gives a polymer–matrix composite exhibiting relative dielectric constant 16 at 1 MHz, whereas the addition of barium titanate to epoxy gives a composite exhibiting relative dielectric constant only 6.5 at 1 MHz [106].

The incorporation of GNP that has been coated with an elastomer [a liquid rubber amine-terminated poly(butadiene-co-acrylonitrile)] is effective for increasing the toughness of the composite [107]. The incorporation of GNP in styrene butadiene rubber enhances the fatigue resistance [108].

The addition of GNP to paraffin (a phase change material, or PCM) increases the thermal conductivity, which is important for the heat transfer rate [109–113]. Thermal property enhancement is similarly obtained for various phase change materials, including paraffin, hexadecane, octadecane [114], and bio-based materials [115, 163′]. The addition of GNP to a polymer improves the flame retardancy [116, 117] and increases the thermal conductivity [117]. However, the GNP addition results in decrease in the amount of phase change material, so that the latent heat storage capacity is decreased [112].

The addition of GNP to a short glass fiber epoxy–matrix composite improves the bond between the glass fiber and the epoxy matrix [118]. The GNP addition can be achieved by adding the GNP to either the matrix resin or the glass fiber surface. This composite is an example of a multi-scale (hierarchical) composite. The combined incorporation of GNP and CNT in epoxy gives a hybrid polymer–matrix composite that is attractive for use as the bipolar plate of a fuel cell [119].

The incorporation of GNP in a carbon matrix made from mesophase pitch is a superior anode material for lithium-ion batteries than the corresponding material without GNP [120]. Both the capacity and cycle life are enhanced. The improvement is attributed to the increased electrical conductivity due to the GNP.

The incorporation of GNP in aluminum by powder metallurgy (500 MPa consolidation, followed by sintering at 600 °C) gives a metal–matrix composite. The compressive strength and hardness increase, while the density decreases as the GNP content increases [121]. However, the presence of GNP activates the corrosion of aluminum in the composite [122, 123].

The addition of GNP to wood (high-density fiberboard) reduces the emission rate of volatile organic compounds (VOCs) and formaldehyde (due to the sorption of these substances by GNP) and increases the thermal conductivity [124, 125]. The incorporation of nanoscale iron oxide (Fe_3O_4) in RGO provides a material for the adsorption of contaminants such as amaranth [126].

Nanofluids are colloidal suspensions of nanoparticles in a base fluid. Nanofluids involving dispersed GNP are attractive for ink-jet printing [127], electrophoretic deposition [127], environmental [128, 129], and thermal [70, 130] applications. GNP [131] is effective as a catalyst support.

The TIM performance of the GNP paste is comparable to that of the carbon black paste, in spite of the higher thermal conductivity of the former [70]. This is because of the high conformability of the carbon black paste. The high conformability of carbon black stems from the fact that carbon black is in the form of porous aggregates of

nanoparticles [132]. This morphology renders squishability and hence conformability to the carbon black. Furthermore, carbon black is less expensive than GNP.

Conclusion

EG refers to graphite that has a degree of separation of a substantial portion of the carbon layers in the graphite. The separation occurs between adjacent carbon layers, but typically not all the carbon layers are separated. The separation may or may not occur throughout the entire plane between the adjacent carbon layers. In case that the separation does not occur throughout the entire plane, the graphite remains intact as a single piece, with local separation of the layers in parts of various planes between carbon layers. The distributed local separation of the layers typically results in a cellular structure, with the wall of each cell typically consisting of multiple carbon layers. The volume is increased and the density is decreased relative to graphite that has not been exfoliated. If the porosity includes open porosity, the specific surface area is also increased. In case that the separation occurs throughout the entire plane, the graphite is separated into multiple pieces. If the number of carbon layers is less than 10, the piece is known as graphene. If the number of carbon layers is 10 or more, the piece is known as GNP, which is commonly prepared by mechanical agitation of EG. The EG exhibits clinginess, due to its cellular structure, but GNP does not.

This review focuses on EG that exhibits a cellular structure and on GNP. The former includes EG compacts, which is obtained by the compaction of multiple pieces of EG in the absence of a binder. Due to the cellular structure and the consequent mechanical interlocking among the pieces of EG, the compact is a monolith in the absence of a binder. In case that the compaction pressure is high, the mechanical locking is strong and a reasonably strong sheet results. This sheet is known as flexible graphite.

The exfoliation process that gives EG exhibiting a cellular structure is associated with a large expansion (typically exceeding 100 times) along the *c*-axis of the graphite. Most commonly, the graphite prior to exfoliation is in the form of flakes. Because of the large expansion along the *c*-axis, the exfoliated flake becomes long in the direction that corresponds to the *c*-axis of the flake prior to exfoliation. As a consequence, the EG made from a graphite flake is known as a worm.

The exfoliation of graphite typically involves the intercalation of graphite to form a GIC, followed by heating of the GIC. Upon heating, the intercalate either vaporizes (due to the relatively low boiling point of the intercalate) or decomposes into smaller molecules, thus causing each intercalate island to expand like a balloon. The sliding of the carbon layers relative to one another enables the balloon wall to stretch as the island expands to form a balloon. Thus, a cellular structure results. For a large amount of expansion during exfoliation, a relatively large size of the intercalate islands is preferred.

The process of exfoliation is accompanied by extensive desorption of the intercalate, so that only a very small portion of the intercalate in the intercalation compound remains after exfoliation. The residual intercalate is strongly held in the EG. The most widely used intercalate species for preparing EG is sulfuric acid. In order to decrease the residual acidity in the expandable graphite (prior to exfoliation), rinsing with water followed by partial neutralization (i.e., deacidification using an alkaline material) is commonly conducted. Yet, the amount of surface residue on the EG is lower if the EG has been subjected to washing by water. The higher concentration of surface residual in the unwashed case causes the relative dielectric constant (50 Hz) of the EG to be 360, compared to the value of 38 for the washed case and the value of 120 for KOH-activated GNP.

An EG compact refers to a compact obtained by the compression of worms such that the pressure is considerably lower than that typically used for the fabrication of flexible graphite. The EG compacts are mechanically weak compared to flexible graphite. However, they exhibit viscous character, out-of-plane electrical/thermal conductivity, and liquid permeability that are much greater than those of flexible graphite. The viscous character stems from the sliding of the carbon layers relative to one another, with the ease of the sliding enhanced by the exfoliation process. High values of the out-of-plane electrical/thermal conductivity are attractive for the bipolar plates of fuel cells.

The EG, flexible graphite, and GNP may be used to form composite materials, with matrices such as polymers, metals, carbon, and cement. Due to its small size, GNP is particularly suitable for use as a filler. Due to their connectivity, EG and flexible graphite are attractive for applications that require electrical or thermal conductivity. The applications of the composites include structural, vibration damping, electrochemical, electromagnetic, and thermal applications.

Compliance with ethical standards

Conflict of Interest The author declares that she has no conflict of interest.

References

1. Chung DDL (1987) Exfoliation of graphite. J Mater Sci 22(12):4190–4198. doi:10.1007/978-1-4684-8267-6_4
2. Boehm H (2010) Graphene-how a laboratory curiosity suddenly became extremely interesting. Angew Chem Int Ed 49(49): 9332–9335

3. Ahmadi-Moghadam B, Taheri F (2014) Effect of processing parameters on the structure and multi-functional performance of epoxy/GNP-nanocomposites. J Mater Sci 49(18):6180–6190. doi:10.1007/s10853-014-8332-y
4. Inagaki M, Qiu J, Guo Q (2015) Carbon foam: preparation and application. Carbon 87:128–152
5. Herold A, Petitjean D, Furdin G, Klatt M (1994) Exfoliation of graphite intercalation compounds: classification and discussion of the processes from new experimental data relative to graphite-acid compounds. Mater Sci Forum 152–153(Soft Chemistry Routes to New Materials):281–287
6. Anderson SH, Chung DDL (1984) Exfoliation of intercalated graphite. Carbon 22(3):253–263
7. Anderson SH, Chung DDL (1983) Exfoliation of single crystal graphite and graphite fibers intercalated with halogens. Synth Met 8:343–349
8. Chung DDL (1987) Intercalate vaporization during the exfoliation of graphite intercalated with bromine. Carbon 25(3):361–365
9. Chung DDL (2002) Review graphite. J Mater Sci 37(8): 1475–1489. doi:10.1023/A:1014915307738
10. Dresselhaus MS, Dresselhaus G (2002) Intercalation compounds of graphite. Adv Phys 51(1):1–186
11. Inagaki M, Kang F, Toyoda M (2004) Exfoliation of graphite via intercalation compounds. Chem Phys Carbon 29:1–69
12. Flandrois S, Hauw C, Mathur RB (1989–1990) Charge transfer in acceptor graphite intercalation compounds. Synth Met 34(1–3):399–404
13. van Heerden X, Badenhorst H (2015) The influence of three different intercalation techniques on the microstructure of exfoliated graphite. Carbon 88:173–184
14. Terence MC, Silva EE, Carrio JAG (2014) Electrochemically exfoliated graphene. J. Nano Res 29:29–33
15. Park S, Kim S (2014) Preparation and capacitive property of graphene nanosheets prepared by using an electrostatic method. J Nanosci Nanotechnol 14(10):7784–7787
16. Zhang C, Lv W, Xie X, Tang D, Liu C, Yang Q (2013) Towards low temperature thermal exfoliation of graphite oxide for graphene production. Carbon 62:11–24
17. Mishra AK, Srinath C, Jain PK, Padya B, Chopkar M (2013) Characterization of intermediates in the synthesis of reduced graphene-oxide through sequential de-oxygenation. NanoTrends 14(2):1–9
18. Owens FJ (2015) Raman and surface-enhanced Raman spectroscopy evidence for oxidation-induced decomposition of graphite. Mol Phys 113(11):1280–1283
19. Anderson SH, Chung DDL (1984) Graphite ribbons formed from graphite fibers. Carbon 22(6):613–614
20. Daumas N, Herold A (1969) Relations between phase concept and reaction mechanics in graphite insertion compounds. C R Hebd Seances Acad Sci C 268:373–382
21. Heerschap M, Delavignette P, Amelinckx S (1964) Electron microscope study of interlamellar compounds of graphite with bromine, iodine monochloride and ferric chloride. Carbon 1:235–238
22. Heerschap M, Delavignette P (1967) Electron-microscopy study of the ferric chloride/graphite compound. Carbon 5:383–384
23. Saidaminov MI, Maksimova NV, Sorokina NE, Avdeev VV (2013) Effect of graphite nitrate exfoliation conditions on the released gas composition and properties of exfoliated graphite. Inorg Mater 49(9):883–888
24. Yu K (2011) Preparation of exfoliated graphite by microwave using natural graphite with different particle sizes. Adv Mater Res (Zuerich, Switzerland) 163–167(Pt. 3, Advances in Structures): 2333–2336
25. Zhao Q, Cheng X, Wu J, Yu X (2014) Sulfur-free exfoliated graphite with large exfoliated volume: Preparation, characterization and its adsorption performance. J Ind Eng Chem (Amst Neth) 20(6):4028–4032
26. Sykam Nagaraju, Kar Kamal K (2014) Rapid synthesis of exfoliated graphite by microwave irradiation and oil sorption studies. Mater Lett 117:150–152
27. Huczko A, Dabrowska A, Labedz O, Soszynski M, Bystrzejewski M, Baranowski P, Bhatta R, Pokhrel B, Kafle BP, Stelmakh S, Gierlotka S, Dyjak S (2014) Facile and fast combustion synthesis and characterization of novel carbon nanostructures. Phys Status Solidi B 251(12):2563–2568
28. Tanaike O, Yamada Y, Kodama M, Miyajima N (2012) Exfoliation of graphite by pyrolysis of bromine-graphite intercalation compounds in a vacuum glass tube. J Phys Chem Solids 73(12):1420–1423
29. Kovtyukhova NI, Wang Y, Berkdemir A, Cruz-Silva R, Terrones M, Crespi VH, Mallouk TE (2014) Non-oxidative intercalation and exfoliation of graphite by Bronsted acids. Nat Chem 6(11):957–963
30. Celzard A, Mareche JF, Furdin G (2005) Modelling of exfoliated graphite. Prog Mater Sci 50(1):93–179
31. Chen P, Chung DDL (2013) Viscoelastic behavior of the cell wall of exfoliated graphite. Carbon 61:305–312
32. Wang A, Chung DDL (2014) Dielectric and electrical conduction behavior of carbon paste electrochemical electrodes, with decoupling of carbon, electrolyte and interface contributions. Carbon 72:135–151
33. Bardhan KK, Wu JC, Culik JS, Anderson SH, Chung DDL (1980) Kinetics of intercalation and desorption in graphite. Synth Met 2:57
34. Asghar HMA, Hussain SN, Sattar H, Brown NW, Roberts EPL (2014) Environmentally friendly preparation of exfoliated graphite. J Ind Eng Chem (Amst Neth) 20(4):1936–1941
35. Liu D, Liang J (2014) Preparation of expandable graphite by ozone oxidation method. Adv Mater Res (Durnten-Zurich, Switzerland) 1051(Applied Engineering Decisions in the Context of Sustainable Development):121–124
36. Zhao J, Li X, Guo Y, Ma D (2014) Preparation and microstructure of exfoliated graphite with large expanding volume by two-step intercalation. Adv Mater Res (Durnten-Zurich, Switzerland) 852:101–105
37. Zhao J, Li X, Guo Y, Ma D, Li Y (2014) Microstructure and millimeter-wave attenuation performance of exfoliated graphite with different expanding volume. Key Eng Mater 609–610(Micro-Nano Technology XV):3–7
38. Zhao J, Li X, Guo Y, Ma D (2014) Preparation and microstructure of exfoliated graphite with large expanding volume by two-step intercalation. Adv Mater Res (Durnten-Zurich, Switzerland) 852(Material Science and Advanced Technologies in Manufacturing):101–105
39. Hong X, Chung DDL (2015) Exfoliated graphite with relative dielectric constant reaching 360, obtained by exfoliation of acid-intercalated graphite flakes without subsequent removal of the residual acidity. Carbon 91:1–10
40. Ndlovu T, Arotiba OA, Sampath S, Krause RW, Mamba BB (2012) Reactivities of modified and unmodified exfoliated graphite electrodes in selected redox systems. Int J Electrochem Sci 7(10):9441–9453
41. Wei XH, Liu L, Zhang JX, Shi JL, Guo QG (2010) The preparation and morphology characteristics of exfoliated graphite derived from $HClO_4$-graphite intercalation compounds. Mater Lett 64(9):1007–1009
42. Skowronski JM, Krawczyk P (2010) Improved hydrogen sorption/desorption capacity of exfoliated $NiCl_2$-graphite intercalation compound effected by thermal treatment. Solid State Ionics 181(13–14):653–658

43. Ovsiienko I, Lazarenko O, Matzui L, Brusylovets O, Le Normand F, Shames A (2014) Influence of chemical treatment on the microstructure of nanographite. Phys Status Solidi A 211(12):2765–2772
44. Guadagno L, Raimondo M, Vertuccio L, Mauro M, Guerra G, Lafdi K, De Vivo B, Lamberti P, Spinelli G, Tucci V (2015) Optimization of graphene-based materials outperforming host epoxy matrices. RSC Adv 5(46):36969–36978
45. She Y, Lu Z, Ni M, Li L, Leung MKH (2015) Facile synthesis of nitrogen and sulfur codoped carbon from ionic liquid as metal-free catalyst for oxygen reduction reaction. ACS Appl Mater Interfaces 7(13):7214–7221
46. Mar M, Ahmad Y, Dubois M, Guerin K, Batisse N, Hamwi A (2015) Dual C-F bonding in fluorinated exfoliated graphite. J Fluor Chem 174:36–41
47. Wang G, Sun Q, Zhang Y, Fan J, Ma L (2010) Sorption and regeneration of magnetic exfoliated graphite as a new sorbent for oil pollution. Desalination 263(1–3):183–188
48. Ionov SG, Avdeev VV, Kuvshinnikov SV, Pavlova EP (2000) Physical and chemical properties of flexible graphite foils. Mol Cryst Liquid Cryst Sci Technol A 340(349–54):29
49. Wei XH, Liu L, Zhang JX, Shi JL, Guo QG (2010) Mechanical, electrical, thermal performances and structure characteristics of flexible graphite sheets. J Mater Sci 45:2449–2455. doi:10.1007/s10853-010-4216-y
50. Chung DDL (2000) Flexible graphite for gasketing, adsorption, electromagnetic interference shielding, vibration damping, electrochemical applications, and stress sensing. J Mater Eng Perform 9(2):161–163
51. Chugh R, Chung DDL (2002) Flexible graphite as a heating element. Carbon 40(13):2285–2289
52. Chen P, Chung DDL (2012) Dynamic mechanical properties of flexible graphite made from exfoliated graphite. Carbon 50:283–289
53. Luo X, Chugh R, Biller BC, Hoi YM, Chung DDL (2002) Electronic applications of flexible graphite. J Electron Mater 31(5):535–544
54. Luo X, Chung DDL (1996) Electromagnetic interference shielding reaching 130 dB using flexible graphite. Carbon 34(10):1293–1294
55. Chung DDL (2001) Electromagnetic interference shielding effectiveness of carbon materials. Carbon 39(2):279–285
56. Kitaoka S, Wada M, Nagai T, Osa N, Konno T (2011) Increasing the thermal diffusivity of flexible graphite sheets by superheated steam treatment. J Mater Sci 46(4):1132–1135. doi:10.1007/s10853-010-4991-5
57. Kobayashi M, Toda H, Takeuchi A, Uesugi K, Suzuki Y (2012) Three-dimensional evaluation of the compression and recovery behavior in a flexible graphite sheet by synchrotron radiation microtomography. Mater Charact 69:52–62
58. Chung DDL (2012) Carbon materials for structural self-sensing, electromagnetic shielding and thermal interfacing. Carbon 50:3342–3353
59. Chung DDL, Takizawa Y (2012) Performance of isotropic and anisotropic heat spreaders. J Electron Mater 41(9):2580–2587
60. Rogacheva AE, Kharitonov AP, Vinogradov AS, Teplyakov VV (2010) Gas permeability properties of modified membranes based on exfoliated graphite. Desalin Water Treat 14(1–3):192–195
61. Chen P, Chung DDL (2014) Thermal and electrical conduction in the compaction direction of exfoliated graphite and their relation to the structure. Carbon 77:538–550
62. Chung DDL (2014) Interface-derived extraordinary viscous behavior of exfoliated graphite. Carbon 68:646–652
63. Chen P, Chung DDL (2015) Elastomeric behavior of exfoliated graphite, as shown by instrumented indentation testing. Carbon 81:505–513
64. Fu W, Chung DDL (2001) Vibration reduction ability of polymers, particularly polymethylmethacrylate and polytetrafluoroethylene. Polym Polym Compos 9(6):423–426
65. Muthusamy S, Wang S, Chung DDL (2010) Unprecedented vibration damping with high values of loss modulus and loss tangent, exhibited by cement-matrix graphite network composite. Carbon 48(5):1457–1464
66. Chen P, Chung DDL (2013) Comparative evaluation of cement-matrix composites with distributed versus networked exfoliated graphite. Carbon 63:446–453
67. Filimonov SV, Sorokina NE, Yashchenko NV, Malakho AP, Avdeev VV (2013) Thermal properties of high-porosity monoliths based on exfoliated graphite. Inorg Mater 49(4):340–346
68. Gao L, Tu H (2014) Research on oilfield produced water treatment by moderately compressed exfoliated graphite blocks. Appl Mech Mater 468(Research on Material Engineering and Manufacturing Engineering):53–56
69. Ndlovu T, Arotiba OA, Sampath S, Krause RW, Mamba BB (2011) Electrochemical detection and removal of lead in water using poly(propylene imine) modified re-compressed exfoliated graphite electrodes. J Appl Electrochem 41(12):1389–1396
70. Lin C, Chung DDL (2009) Graphite nanoplatelet pastes versus carbon black pastes as thermal interface materials. Carbon 47(1):295–305
71. Xiang J, Drzal LT (2011) Thermal conductivity of exfoliated graphite nanoplatelet paper. Carbon 49(3):773–778
72. Ferreira CI, Bianchi O, Oviedo MAS, Bof-de-Oliveira RV, Mauler RS (2013) Morphological, viscoelastic and mechanical characterization of polypropylene/exfoliated graphite nanocomposites. Polimeros Ciencia e Tecnologia 23(4):456–461
73. Sykam N, Gautam RK, Kar KK (2015) Electrical, mechanical, and thermal properties of exfoliated graphite/phenolic resin composite bipolar plate for polymer electrolyte membrane fuel cell. Polym Eng Sci 55(4):917–923
74. Valentini M, Piana F, Pionteck J, Lamastra FR, Nanni F (2015) Electromagnetic properties and performance of exfoliated graphite (EG)—thermoplastic polyurethane (TPU) nanocomposites at microwaves. Compos Sci Technol 114:26–33
75. Boehle M, Lafdi K, Zinsser E, Collins P (2010) Exfoliated graphite as a filler to enhance the electromagnetic interference shielding of polymers. J Sci Conf Proc 2(1):3–7
76. Avila AF, Munhoz VC, de Oliveira AM, Santos MCG, Lacerda GRBS, Goncalves CP (2014) Nano-based systems for oil spills control and cleanup. J Hazard Mater 272:20–27
77. Kujawski M, Pearse JD, Smela E (2010) Elastomers filled with exfoliated graphite as compliant electrodes. Carbon 48(9):2409–2417
78. Yu L, Zhang Y, Shang J, Ke S, Tong W, Shen B, Huang H (2012) Electrical and dielectric properties of exfoliated graphite/polyimide composite films with low percolation threshold. J Electron Mater 41(9):2439–2446
79. Yu L, Zhang Y, Tong W, Shang J, Lv F, Chu PK, Guo W (2012) Hierarchical composites of conductivity controllable polyaniline layers on the exfoliated graphite for dielectric application. Composites A 43(11):2039–2045
80. Naderi HR, Mortaheb HR, Zolfaghari A (2014) Supercapacitive properties of nanostructured MnO_2/exfoliated graphite synthesized by ultrasonic vibration. J Electroanal Chem 719:98–105
81. Yang Y, Liu E, Li L, Huang Z, Shen H, Xiang X (2009) Nanostructured MnO_2/exfoliated graphite composite electrode as supercapacitors. J Alloys Compd 487(1–2):564–567
82. Focke WW, Badenhorst H, Ramjee S, Kruger HJ, Van Schalkwyk R, Rand B (2014) Graphite foam from pitch and expandable graphite. Carbon 73:41–50
83. Jana P, Fierro V, Pizzi A, Celzard A (2014) Biomass-derived, thermally conducting, carbon foams for seasonal thermal storage. Biomass Bioenergy 67:312–318

84. Tikhomirov AS, Sorokina NE, Shornikova ON, Morozov VA, Van Tendeloo G, Avdeev VV (2010) The chemical vapor infiltration of exfoliated graphite to produce carbon/carbon composites. Carbon 49(1):147–153
85. Chen P, Chung DDL (2013) Mechanical energy dissipation using cement-based materials with admixtures. ACI Mater J 110(3):279–290
86. Fu X, Chung DDL (1996) Vibration damping admixtures for cement. Cem Concr Res 26(1):69–75
87. Chung DDL (2002) Improving cement-based materials by using silica fume. J Mater Sci 37(4):673–682. doi:10.1023/A:1013889725971
88. Song X, Shi Z, Tan X, Zhang S, Liu G, Wu K (2014) One-step solvent exfoliation of graphite to produce a highly-sensitive electrochemical sensor for tartrazine. Sens Actuators B 197:104–108
89. Ma C, Ma C, Wang J, Wang H, Shi J, Song Y, Guo Q, Liu L (2014) Exfoliated graphite as a flexible and conductive support for Si-based Li-ion battery anodes. Carbon 72:38–46
90. Zhao Q, Meng S, Wang J, Li Z, Liu J, Guo Y (2014) Preparation of solid superacid S_2O_2-8/TiO_2-exfoliated graphite (EG) and its catalytic performance. Ceramics Int 40(10 Part B):16183–16187
91. Ischenko EV, Matzui LY, Gayday SV, Vovchenko LL, Kartashova TV, Lisnyak VV (2010) Thermo-exfoliated graphite containing CuO/$Cu_2(OH)_3NO_3$:(Co^{2+}/Fe^{3+}) composites: preparation, characterization and catalytic performance in CO conversion. Materials 3:572–584
92. Savchenko DV, Ionov SG, Sizov AI (2010) Properties of carbon-carbon composites based on exfoliated graphite. Inorg Mater 46(2):132–138
93. Sharma M, Chung DDL (2015) Solder-graphite network composite sheets as high-performance thermal interface materials. J Electron Mater 44(3):929–947
94. Leong C, Aoyagi Y, Chung DDL (2006) Carbon black pastes as coatings for improving thermal gap-filling materials. Carbon 44(3):435–440
95. Wang H, Liu Z, Chen X, Han P, Dong S, Cui G (2011) Exfoliated graphite nanosheets/carbon nanotubes hybrid materials for superior performance supercapacitors. J Solid State Electrochem 15(6):1179–1184
96. Kim M, Hwang S, Kim B, Baek J, Shin H, Park HW, Park Y, Bae I, Lee S (2014) Modeling, processing, and characterization of exfoliated graphite nanoplatelet-nylon 6 composite fibers. Composites B 66:511–517
97. Karevan M, Kalaitzidou K (2013) Understanding the property enhancement mechanism in exfoliated graphite nanoplatelets reinforced polymer nanocomposites. Compos Interfaces 20(4):255–268
98. Duguay AJ, Kiziltas A, Nader JW, Gardner DJ, Dagher HJ (2014) Impact properties and rheological behavior of exfoliated graphite nanoplatelet-filled impact modified polypropylene nanocomposites. J Nanopart Res 16(3):2307/1–2307/11
99. King JA, Via MD, Morrison FA, Wiese KR, Beach EA, Cieslinski MJ, Bogucki GR (2012) Characterization of exfoliated graphite nanoplatelets/polycarbonate composites: electrical and thermal conductivity, and tensile, flexural, and rheological properties. J Compos Mater 46(9):1029–1039
100. Alzari V, Mariani A, Monticelli O, Valentini L, Nuvoli D, Piccinini M, Scognamillo S, Bon SB, Illescas J (2010) Stimuli-responsive polymer hydrogels containing partially exfoliated graphite. J Polym Sci A 48(23):5375–5381
101. Patsidis AC, Kalaitzidou K, Psarras GC (2014) Graphite nanoplatelets/polymer nanocomposites: thermomechanical, dielectric, and functional behavior. J Therm Anal Calorim 116(1):41–49
102. Al-Ghamdi AA, Al-Hartomy OA, Al-Solamy F, Al-Ghamdi AA, El-Tantawy F (2013) Electromagnetic wave shielding and microwave absorbing properties of hybrid epoxy resin/foliated graphite nanocomposites. J Appl Polym Sci 127(3):2227–2234
103. Kim M, Yan J, Joo K, Pandey JK, Kang Y, Ahn S (2013) Synergistic effects of carbon nanotubes and exfoliated graphite nanoplatelets for electromagnetic interference shielding and soundproofing. J Appl Polym Sci 130(6):3947–3951
104. Shui X, Chung DDL (1997) Nickel filament polymer-matrix composites with low surface impedance and high electromagnetic interference shielding effectiveness. J Electron Mater 26(8):928–934
105. He F, Lam K, Fan J, Chan LH (2014) Improved dielectric properties for chemically functionalized exfoliated graphite nanoplates/syndiotactic polystyrene composites prepared by a solution-blending method. Carbon 80:496–503
106. Patsidis AC, Kalaitzidou K, Psarras GC (2012) Dielectric response, functionality and energy storage in epoxy nanocomposites: barium titanate vs. exfoliated graphite nanoplatelets. Mater Chem Phys 135(2–3):798–805
107. Cho D, Hwang JH (2013) Elastomeric coating of exfoliated graphite nanoplatelets with amine-terminated poly(butadiene-co-acrylonitrile): characterization and its epoxy toughening effect. Adv Polymer Technol 32(4):21366/1–21366/8
108. Song SH, Jeong HK, Kang YG (2010) Preparation and characterization of exfoliated graphite and its styrene butadiene rubber nanocomposites. J Ind Eng Chem (Amst Neth) 16(6):1059–1065
109. Jeong S, Chang SJ, We S, Kim S (2015) Energy efficient thermal storage montmorillonite with phase change material containing exfoliated graphite nanoplatelets. Solar Energy Mater Solar Cells 139:65–70
110. Wu C, Pu N, Liao C, Wu B, Liu Y, Ger M (2015) High-electrical-resistivity thermally-conductive phase change materials prepared by adding nanographitic fillers into paraffin. Microelectron Eng 138:91–96
111. Mallow A, Abdelaziz O, Kalaitzidou K, Graham S (2012) Investigation of the stability of paraffin-exfoliated graphite nanoplatelet composites for latent heat thermal storage systems. J Mater Chem 22(46):24469–24476
112. Huang J, Wang TY, Wang CH, Rao ZH (2011) Exfoliated graphite/paraffin nanocomposites as phase change materials for thermal energy storage application. Mater Res Innov 15(6):422–427
113. Xiang J, Drzal LT (2011) Investigation of exfoliated graphite nanoplatelets (xGnP) in improving thermal conductivity of paraffin wax-based phase change material. Solar Energy Mater Solar Cells 95(7):1811–1818
114. Jeong S, Jeon J, Chung O, Kim S, Kim S (2013) Evaluation of PCM/diatomite composites using exfoliated graphite nanoplatelets (xGnP) to improve thermal properties. J Therm Anal Calorim 114(2):689–698
115. Jeong S, Chung O, Yu S, Kim S, Kim S (2013) Improvement of the thermal properties of Bio-based PCM using exfoliated graphite nanoplatelets. Solar Energy Mater Solar Cells 117:87–92
116. Idumah CI, Hassan A, Affam AC (2015) A review of recent developments in flammability of polymer nanocomposites. Rev Chem Eng 31(2):149–177
117. Inuwa IM, Hassan A, Wang D, Samsudin SA, Mohamad Haafiz MK, Wong SL, Jawaid M (2014) Influence of exfoliated graphite nanoplatelets on the flammability and thermal properties of polyethylene terephthalate/polypropylene nanocomposites. Polym Degrad Stab 110:137–148
118. Pedrazzoli D, Pegoretti A, Kalaitzidou K (2014) Synergistic effect of exfoliated graphite nanoplatelets and short glass fiber on the mechanical and interfacial properties of epoxy composites. Compos Sci Technol 98:15–21
119. Kim M, Kang G, Park HW, Park Y, Park Y, Yoon KH (2012) Design, manufacturing, and characterization of high-performance lightweight bipolar plates based on carbon nanotube-

exfoliated graphite nanoplatelet hybrid nanocomposites. J Nanomater 2012:115
120. Yang Y, Wang C, Chen M, Shi Z, Zheng J (2010) Facile synthesis of mesophase pitch/exfoliated graphite nanoplatelets nanocomposite and its application as anode materials for lithium-ion batteries. J Solid State Chem 183(9):2116–2120
121. Sherif EM, Latief FH, Junaedi H, Almajid AA (2012) Influence of exfoliated graphite nanoplatelets particles additions and sintering temperature on the mechanical properties of aluminum matrix composites. Int J Electrochem Sci 7(5):4352–4361
122. Latief FH, Sherif EM, Almajid AA, Junaedi H (2011) Fabrication of exfoliated graphite nanoplatelets-reinforced aluminum composites and evaluating their mechanical properties and corrosion behavior. J Anal Appl Pyrolysis 92(2):485–492
123. Sherif EM, Almajid AA, Latif FH, Junaedi H (2011) Effects of graphite on the corrosion behavior of aluminum-graphite composite in sodium chloride solutions. Int J Electrochem Sci 6(4):1085–1099
124. Kim J, Lee J, Choi Y, Kim S, Moon HJ, Yoon D (2013) Confirmation of the performance of exfoliated graphite nanoplatelets for pollutant reduction rate on wood panel. J Compos Mater 47(8):1039–1044, 6
125. Lee J, Kim J, Kim S, Kim JT (2013) Thermal extractor analysis of VOCs emitted from building materials and evaluation of the reduction performance of exfoliated graphite nanoplatelets. Indoor Built Environ 22(1):68–76, 9
126. Jiang H, Chen P, Zhang W, Luo S, Luo X, Au C, Li M (2014) Deposition of nano Fe_3O_4mZrO_2 onto exfoliated graphite oxide sheets and its application for removal of amaranth. Appl Surf Sci 317:1080–1089
127. Rider AN, An Q, Thostenson ET, Brack N (2014) Ultrasonicated-ozone modification of exfoliated graphite for stable aqueous graphitic nanoplatelet dispersions. Nanotechnology 25(49):495607/1–495607/12
128. Ion I, Sirbu F, Ion AC (2015) Thermophysical investigations of exfoliated graphite nanoplatelets and active carbon in binary aqueous environments at different temperatures. J Mater Sci 50(2):587–598. doi:10.1007/s10853-014-8616-2
129. Ion AC, Alpatova A, Ion I, Culetu A (2011) Study on phenol adsorption from aqueous solutions on exfoliated graphitic nanoplatelets. Mater Sci Eng B 176(7):588–595
130. Park EJ, Park SD, Bang IC, ParkY Park HW (2012) Critical heat flux characteristics of nanofluids based on exfoliated graphite nanoplatelets (xGnPs). Mater Lett 81:193–197
131. Do I, Drzal LT (2014) Ionic liquid-assisted synthesis of Pt nanoparticles onto exfoliated graphite nanoplatelets for fuel cells. ACS Appl Mater Interfaces 6(15):12126–12136
132. Lin C, Chung DDL (2007) Effect of carbon black structure on the effectiveness of carbon black thermal interface pastes. Carbon 45(15):2922–2931